Kuwait J. Sci. **46 (4)** pp. 66-74, 2019

Experimental investigation of maximum stress concentrations in a femur bone by photoelastic approach

Bruce Ralphin Rose. J*

Dept. of Mechanical Engineering, Anna University Regional Campus, Tirunelveli-627007, India

**Corresponding author: bruce@auttvl.ac.in*

Abstract

Progress in experimental stress analysis methods furthers the understanding of stress distribution in bone structures that are essential to know when performing successful implants. Biomechanics requires professional methodologies to solve complex problems. This includes the measurement of physical reactions caused by loads that are impractical in nature. The maximum stress distribution behavior of a human femur bone under the action of startling loads caused by accidents/sporting activities was investigated through the photoelastic method. The experiments were carried out using a circular Polariscope at different input loads and boundary conditions. The stress concentration factor was computed through fringe orders that are related to the stresses obtained from the model. A 2D-scale model of the femur bone was developed with an acrylic material to capture the stress field by optical illumination method. Photoelastic stress analysis revealed the maximum shear stress in the plane of the model and the principal stress difference with high reliability. The nominal stress magnitudes were computed from the fringe order by supplementary data and numerical analysis. State of stress in the femur at different instances was captured through multiple oblique views of the isochromatic fringes. The novel fringe interpretation method facilitated the identification of suitable material for implants with a high factor of safety at actual loading conditions.

Keywords: Biomechanics; femur bone; fracture; photo elasticity; polarized light.

1. Introduction

From the late 1930s, Photoelastic analysis has been implemented on bones and biomedical implants along with other engineering systems (Roesler, 1987). Huang *et al*. (2012) stated that bone adapts to applied loads at various circumstances, which reduces possible damages through unknown physiochemical mechanisms. Previously, immense theoretical and practical significance were given to bone studies by relating it to natural welding and consolidation processes.

Photoelastic analysis related to the mechanical behavior of materials to compute the maximum stress distribution in bone implants is a complex assignment because of its rate-dependent anisotropic properties. Since the biological tissues that exist inside the femur are nonhomogeneous and anisotropic in nature, the mechanical properties should be characterized based on the direction of loading and symmetry (Rodrigues *et al*., 1999). Hence, in the present investigation, the femur anatomical configuration is studied through a novel simplified hypothesis by assuming material isotropy and stepped loading sequences. The isotropy assumption is valid for the photoelastic material as well as the femur for the unidirectional loading case according to the inferences obtained from relative works. Brian (2014) studied the stress-induced birefringence property. It can be used to analyze the failure stresses in a 3D femur through the photoelastic material that exhibits isotropic characteristics. The nominal stress magnitudes are computed from the fringe order by supplementary data obtained from similar research and by numerical analysis.

1.1 Photoelastic modeling in bioengineering

Photoelastic stress investigation can be used either qualitatively or quantitatively for applied or molded-in stress cases. Then, the fringe orders are related directly to the stress distribution in the model through a fundamental relationship known as stress-optic law. The fringe patterns offer generous information regarding the stress distribution at different loading instances. The fringes adjacent to the inner boundary of the sample represent tensile stresses and the outside edge reflects the compressive stresses (Rodrigues *et al*., 1999). If the

inner and outer boundary fringes are not apparent, then a simple numerical computation can be used to determine the tensile or compressive limits.

The photoelastic method offers several advantages as compared to the Finite Element Analysis (FEA) regardless of model manufacturing difficulties. The theory of models can be easily adopted to relate the stresses obtained from the model to the prototype (Ralph & Amber, 2015). There are some significant points regarding the photoelastic method that must be noted:

- The peak stresses and stress concentrations around the notches can be determined accurately to conclude the causes of failure.
- The overstressed and under stressed regions of bones are identified instantaneously with complete field data acquisition.
- The stress measurements are unaffected by humidity and other environmental factors.
- The influence of coatings on the principal stresses and its directions at any point on the model can be measured at different loading conditions.
- An understanding of yielding phenomenon and redistribution of strains in plastic range is needed (see www.micro-measurements. com).

1.2 Femur bone and its failure

The femur bone is the primary bone of the leg that supports and balances the spine system in the course of physical activities (see www.aaos.org). In human anatomy, the femur is the largest bone structure that requires more power to break it, especially for compressive loads. The femurs carry the a major portion of an individual's body weight and loads during various physical activities. Femur length is typically 26% of the total height of a person, which is a useful ratio in the study of anthropology (see www.dolcera.com).

1.3 Inferences from the previous studies

The inferences gained from the related research can be summarized as follows:

- The photoelastic experimental methods are widely used for the analysis of displacements and the stress distributions of a human femur.
- Photoelasticity is an optical communication between the orthopedic engineer and an individual who needs specific implants.
- Photo elasticity provides a complete mapping of shear strain distribution, and it is usually independent of elastic constants.
- Samuel (2002) confirmed that a minute femoral neck-shaft angle is a key safety factor for an unsteady tension type of fracture.

2. Modeling of bone structure

In this study, a femur bone from the right side of a human body was considered. The photoelastic investigation was done for two different loading cases: vertical loading on the femoral head and a horizontal point load on the femoral shaft. These two cases typically represent a fall from heights or an impact caused by an accident. The stepped loading input that spans less than a second through the electronic actuators will be given to replicate the dynamic loading conditions. The average length of an adult male femur is about 48 cm, and the mid-shaft diameter is 2.84 cm. Hence, a prototype-to-model scaling ratio 1:6 was maintained during the experiments conducted in a circular Polariscope facility (Figure 1).

The actual femur structure has the potential to withstand up to 30 times the weight of an individual (both sides together). Therefore, the applied loads were also scaled in proportion with the model dimensions. The scaling was done such that the maximum load input was assumed about 200 N through stepped loading method. This is allowed for the observation of photoelastic fringes in terms of isoclinics and isochromatics (Liming *et al*., 2004). Isoclinic fringes are the family of dark regions that represents the loci of steady principal stress distributions. However, the isochromatic fringes provide the principal stress magnitudes and are colored in nature as viewed through white light.

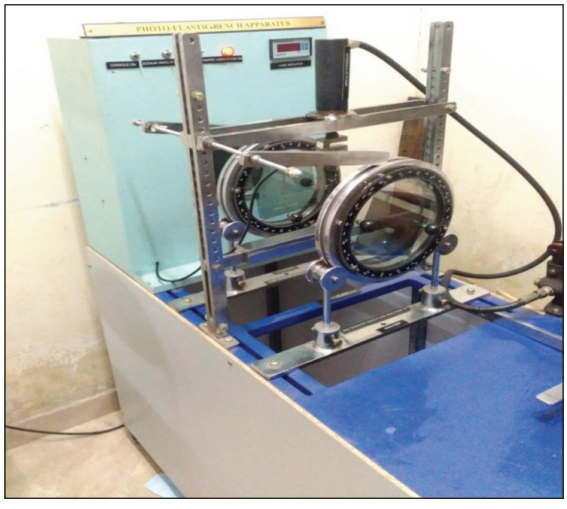

Fig. 1. Circular Polariscope facility with load cells

2.1 Specimen preparation

A 2D model of a femur bone was prepared for the photoelastic analysis in order to compute the stress concentration factor at different loading conditions. Polymethyl-Methacrylate (PMMA) is an amorphous thermoplastic which is optically transparent, impassive to moisture, and offers a high strength-to-weight ratio. Since the maximum stress field at different loading instances was the primary concern, this cost-effective cast acrylic material was used instead of Gelatin or other polymer resins. However, stiffer birefringent polymer resins should be selected for detailed characterization to the molecular level biomechanics. The acrylic raw sheet measuring 250 mm × 250 mm × 8 mm was used to prepare the 2D model of the femur (Figure 2).

Table 1. Acrylic sheet properties of the photoelastic model

Sl.No	Property	Values
1.	Density (g/cm³)	1.18
2.	Melting Temp (°C)	130-140
3.	Max Operating Temp (°C)	65-93
4.	Hardness, Rockwell	M80 – M100
5.	Tensile Strength (psi)	8,000 – 11,000
6.	Light Transmission, minimum (%)	92
7.	Refractive Index	1.48 -1.50

2.2 Boundary conditions

The computation of stress fields in the cortical and trabecular bones caused by the different loads was evaluated by applying suitable boundary conditions. Initially, the proximal femur was mounted onto the photoelastic test bench, and the hydraulic loading point was located on the femoral head. Based on the tensile strength of the PMMA material, the applied normal loads were gradually increased from 50 N to 200 N. These loading measures were assumptions of possible loads during various sports activities or during accidents. The ends are simply supported on the head and patella. Furthermore, the loads were restricted to 50 N to 150 N because of the minimum cross sectional area at the mid-shaft. The oblique fracture can occur by a simple microscopic slip at the mid-shaft region and hence the femoral implants should be customized with full stress field information.

3. Results and discussion

The circular Polariscope arrangement presented in Figure 4 is equipped with monochromatic and white light sources. Temporary double refraction is the primary optical property necessary for the transparent materials

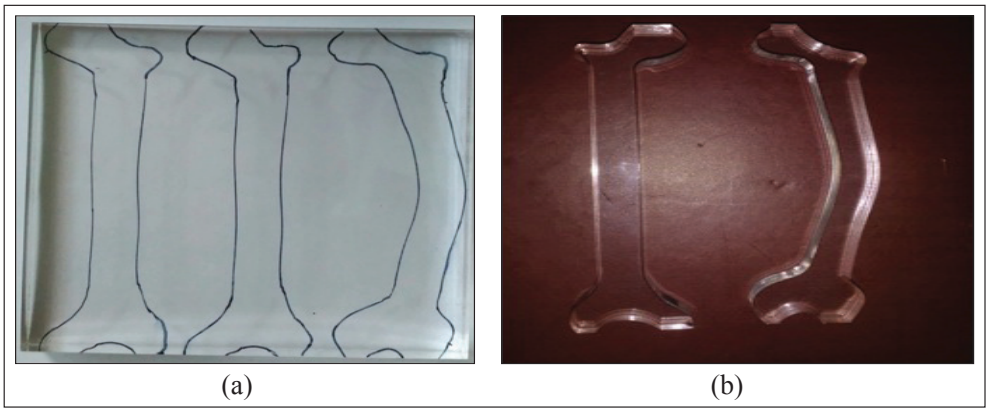

(a) (b)

Fig. 2. femur model (a) marked in acrylic sheet, (b) cut piece of femur model

The 1:6 ratio scaled model is marked in the Acrylic sheet and the laser cutting process is used for good surface finishing at the edges. Here, in the mid-section of femoral shaft a typical 13^0 bend is included to resemble the actual bone structure (Jaime *et al*., 2013). Further, a metal cap is prepared to fix the model firmly in the photoelastic bench without any slipping. Bone is a typical example of an inherent composite material because of its differential properties at various locations. In this analysis, it was assumed to be homogeneous in nature (Nithin *et al*., 2015; Yousif & Aziz, 2012). Table 1 shows the properties of the photoelastic model that was prepared from the acrylic sheet.

while being subjected to stresses or deformations (Dragos *et al*., 2006). Orthopedic implants should be prepared with the detailed stress field information to minimize the probabilistic failure of a femoral shaft in the safe life period. The applied forces should closely replicate the prototype loading while the experiments are conducted.

Starting with the unloaded femur model, the load increments offered fringes especially at highly stressed regions. When the load was increased, brand new fringes began to appear, and the former fringes moved towards the region of minimum stress concentration. The fringes were generated in the highly stressed regions of the model in proportion to the incremental loads. It moved towards the less stressed regions until peak loading was reached. Then the fringe orders were related to the stress in the model by means of a simple relationship called as the stress-optic law (Rodrigues *et al*., 1999). This novel fringe interpretation method helped to identify a suitable material for implants that would have a high safety factor at various actual loading conditions. The values of fringe orders corresponding to various fringe colors are listed in Table 2.

Table 2. Fringe order values

Fringe Color	Fringe Order (r)
Black	0
Yellow	0.6
Red or Pink	0.9
Purple	1

3.1 Results for trabecular bone under straight down load on the neck

A fringe pattern in the trabecular (spongy) bone was initially observed by applying stepped loads vertically on the femur head. The fringe orders corresponding to each incremental load were captured and the nominal and maximum stresses values in the model were tabulated (Sandeep & Saroj, 2014).

In this study, the isochromatic and isoclinic fringe patterns corresponding to 50 N, 100 N, 150 N and 200 N of loads were illustrated to read the topographical map of the stress pattern in the femur. Figure 3 shows the isochromatic and isoclinic fringe patterns corresponding to 50 N and 100 N of the vertical load that was applied on the femur head. The boundary conditions for the straight down load case were that the trabecular bone knee joint was fixed ($U_x = U_y = U_z = 0$). The loads were applied vertically along the y-axis. Furthermore, the offset loading was also done to observe the changes in the location of maximum stress at different head and neck loading conditions.

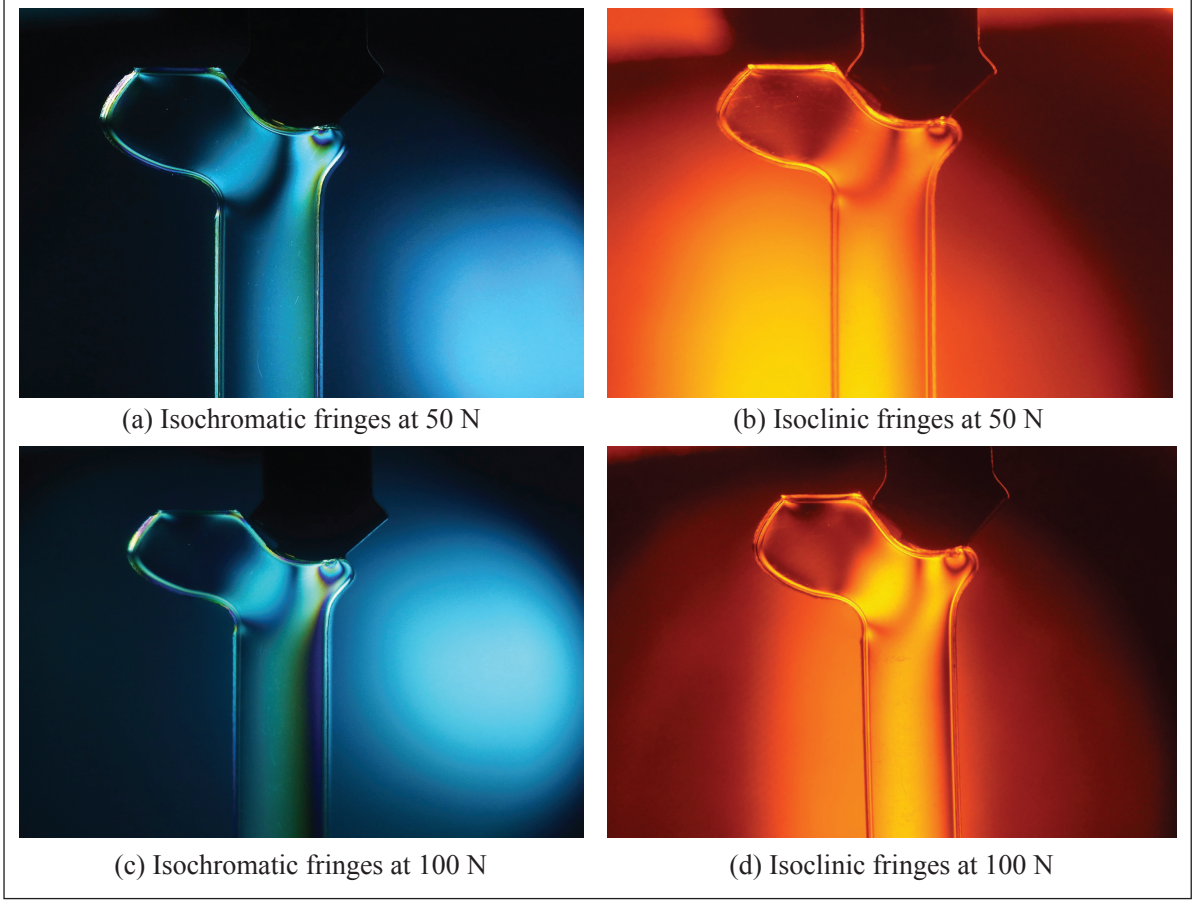

(a) Isochromatic fringes at 50 N

(b) Isoclinic fringes at 50 N

(c) Isochromatic fringes at 100 N

(d) Isoclinic fringes at 100 N

Fig. 3. Fringe patterns for trabecular bone under vertical load case (at neck)

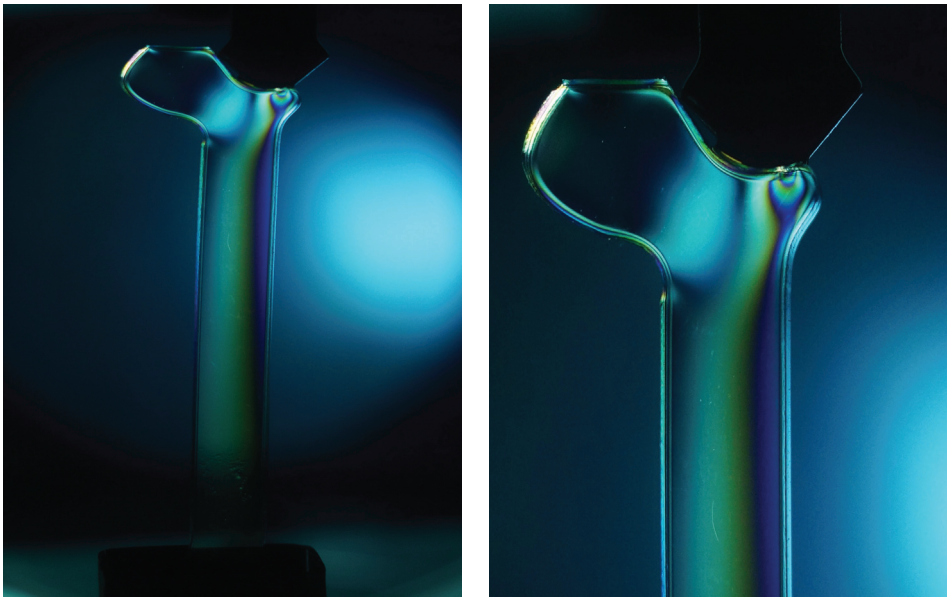

(a) Isochromatic fringes at 150 N (b) Zoom view of fringes at 150 N

Fig. 4. Fringe patterns for Trabecular bone under vertical load of 150 N (at neck)

4. Photoelastic Stress Analysis

Photoelastic fringes include two groups: isoclinics and isochromatics. They assign principal stress directions and magnitudes, respectively. The dark regions are loci of invariable principal stress directions (isostatics) called isoclinic fringes (Liming *et al*., 2004) (Figure 3(b) and 3(d)). The birefringence was observed through the circular Polariscope and plane Polariscope for the compression loading. This was done by rotating the polarized light field. The principal stress magnitudes were computed through the isochromatic fringe patterns with adequate quality (Figure 3(a) and 3(c)). However, in the course of experimental mechanics with crystal level investigation, the quality of the isochromatic recording should meet the biomedical industry standards. A simple numerical calculation can be used to evaluate the maximum stress value for different load inputs as follows:

Step 1

Total number of fringe, $N = n + (1 - r)$ (1)

Here, r Fringe order; - Number of fringes

Step 2

Nominal stress, $\sigma_{nom} = \frac{P}{w * t}$ N/mm^2, (2)

Where, P - Actual load applied; t - Thickness in *mm*; w - Width of section in *mm*

Step 3

Fringe factor, $F_\sigma = \frac{8}{\pi * w} * \left(\frac{P}{n}\right)$ (3)

Step 4

Maximum stress, $\sigma_{\max} = \frac{F_\sigma * N}{t}$ N/mm^2 (4)

For the vertical load applied on the neck, the fringe factor for the 50 N load case was computed as 3.12. For the 100 N loads, it was increased to 8.33. Therefore, the maximum stresses corresponding to 50 N and 100 N loads were 1.72 N/mm^2 and 3.12 N/mm^2, respectively. Figure 4 also shows the fringe patterns for the trabecular bone under a vertical load of 150 N that was applied at the femur neck. Continuing to increase the load on the model produces supplementary relative retardation and the red color is extinguished from the isochromatic fringe pattern as highlighted in Figure 4 (b).

4.1 Results for trabecular bone under straight-down load on the head

The maximum stress distribution for the trabecular bone under a straight-down load on the head is also investigated at different loading conditions to compute the influence of offset loading on the femur. The tissue behavior can also be investigated by preparing the model with different birefringence (the refractive index based on polarization) properties like gelatin-based materials. Figure 5 shows the isoclinic and isochromatic fringes for the spongy bone subjected to 100 N and 150 N of compressive loads that were applied on the femur head.

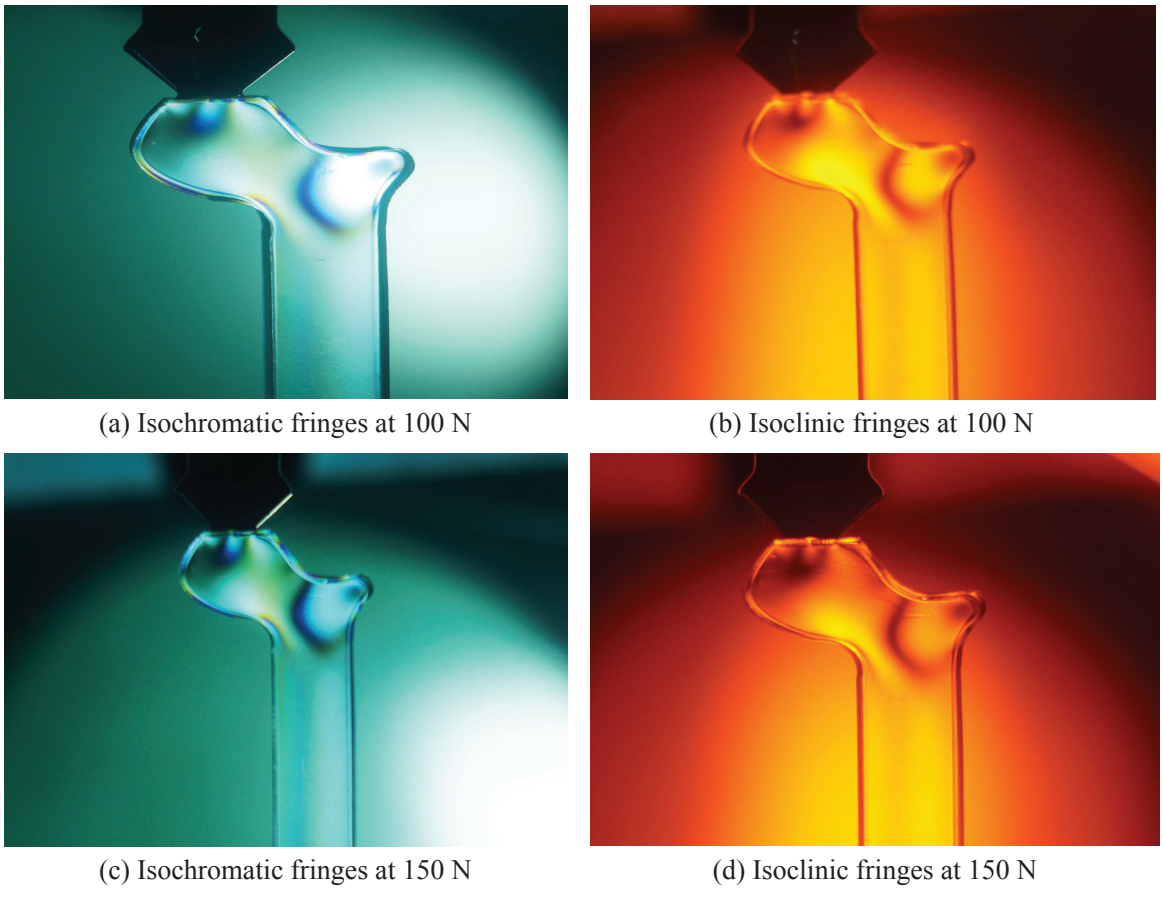

(a) Isochromatic fringes at 100 N

(b) Isoclinic fringes at 100 N

(c) Isochromatic fringes at 150 N

(d) Isoclinic fringes at 150 N

Fig. 5. Fringe patterns for trabecular bone under vertical load case (at head)

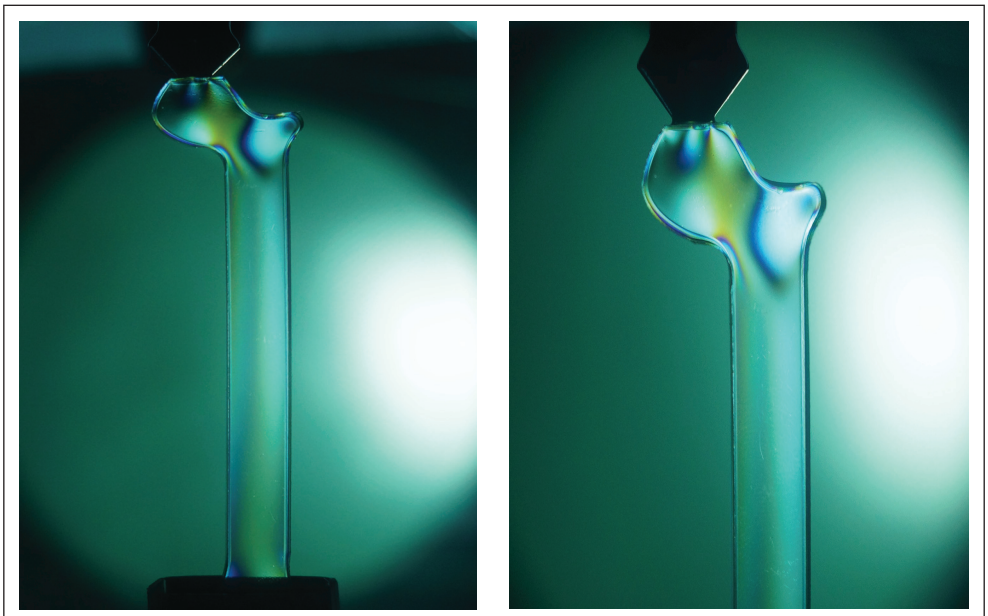

(a) Isochromatic fringes at 200 N

(b) Zoom view of fringes at 200 N

Fig. 6. Isochromatic fringes of femur under vertical load of 200 N (at head)

When a vertical force on the femoral head creates unfavorable stress concentrations in the epiphyseal region, the load offset initiates the bending moment in the entire femur section. Figures 5(a) and (c) present the isochromatic fringes with a relatively higher retardation for incremental wavelengths. It can be observed from the isoclinics in Figures 5(b) and (d) that the first principal stress concentration is around the distal region of the subtrochanter. It is further intensified with incremental loads (Sandeep & Saroj, 2014). This untreated model data can be utilized to minimize the fracture of orthopedically treated bones by providing adequate stiffness to nails or joint materials. As the load increases further, the relative retardation attains a level at which it is twice the wavelength of the violet by quenching the color red for the second time (Figure 6). In addition, as the load increases from 150 N to 200 N, the fringe cycle is repeating at finite loading intervals. Here, the maximum stress corresponding to 200 N load is 6.42 N/mm^2.

4.2 Results for external loading on the femoral shaft

In the vertical loading cases (both femoral head and neck), the maximum deformation obtained in the femur ball bone was about 0.341 mm. This caused a comminute fracture on the untreated femur head as the stress intensity is increased. The nature of impact is also an essential factor because normal activities, like walking and jumping, would not intensify such stresses in the epiphyseal region. The isochromatic fringes for the external loading on the femoral shaft are presented in Figure 7.

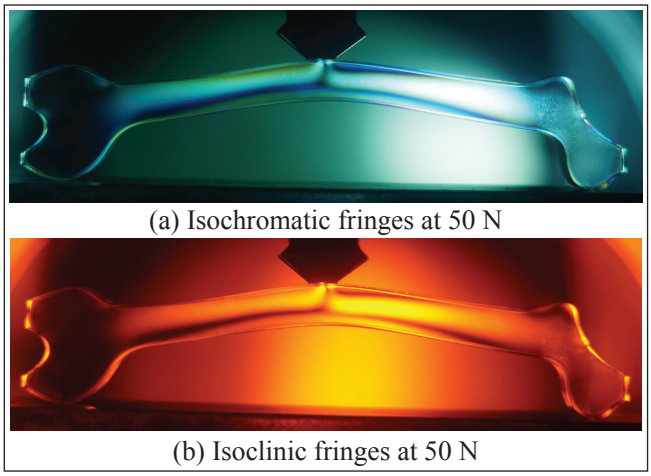

(a) Isochromatic fringes at 50 N

(b) Isoclinic fringes at 50 N

Fig. 7. Fringe patterns of femoral shaft for external load of 50 N

The external loading on the femoral shaft resulted in an oblique fracture, but the minimum deformation which occurred in the bottom section refers lateral condyle. However, a microscopic slip is sufficient to initialize the oblique fracture because the distinctive isoclinic fringes indicate a region of high principal stress direction extending up to the cortical boundary of the femur (Figure 7 (b)). The middle region of the femoral shaft is highly vulnerable in motor vehicle collisions and sporting accidents. Hence, a lateral support with comparatively higher stiffness is mandatory for the treated bones to have a superior medical interface. Figure 8 shows the fringe patterns of the femoral shaft for external load of 100 N. Here, the successive complete color cycle of the fringes can be observed while compared with Figure 7 (a).

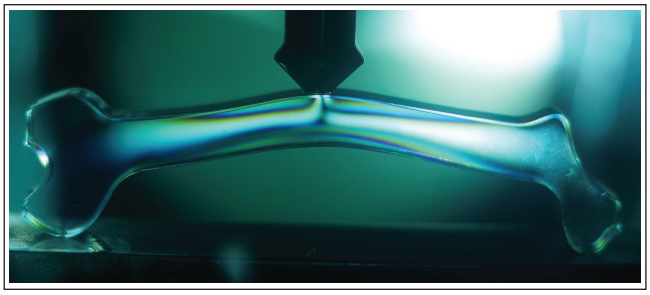

Fig. 8. Isochromatic fringe patterns of femoral shaft for external load of 100 N

5. Conclusions

The determination of the stress concentration factor is extremely essential with all bone implants. An advantage of the photoelastic method is that the stress distribution can be visualized in proportion to the applied loads, and it allows the identification of weak points on the femur. A simple numerical calculation is sufficient to determine the stress distributions through the fringe factor. This can be a validating mechanism for results obtained by finite element analysis. Correct loading and boundary conditions are paramount in order to have the appropriate fringe orders against the applied loads. The highest stress concentration factor of about 2.61 was obtained around the neck of the femur bones at vertical loading because of the reduced radius in this section. In the practice of bone implants, the stress concentration factor plays a vital role in the customization of the stiffness and strength requirements of rod and nails, which is also related to the radius of bone shaft and ball. Scaled dimensions of the model are also considerable factors to match the experimental results with the original femur bone.

In the case of external loading on the femoral shaft, the computed stress concentration factor was about 3.06. The impact loads in association with the kinematic actions of knee joints resulted in an oblique fracture easily irrespective of age group. Hence, the stress intensity of a femur should be completely mapped to ensure reliable and successful orthopedic implants.

References

American Academy of Orthopaedic Surgeons. (2015). Treatment of pediatric diaphyseal femur fractures evidence-based clinical practice guideline, 7-32. Retrieved on DATE:29/10/2018 from www.aaos.org.

Dragoş P., Gherghina, G., Tudor, M. & Tarnita, D. (2006). A 3D graphical modelling method for human femur bone. Journal of Industrial Design and Engineering Graphics, **1**(2): 37-40.

Haughton, S. (2002). Images from waves-Photoelastic modelling of bones", Irish Journal of Medical Science, **172**(4): 209-213.

Huang B.W, C.H. Chang, F.S. Wang, A.D. Lin, Y.C. Tsai, M.Y. Huang, & J.G. Tseng, (2012). Dynamic Characteristics of a Hollow femur, Life Science Journal, **9**(1): 723-726.

Jaime Horta, Ana Leonor Rivera, Agustin de la isla, Adrian oskam, Victor m. castano, (2013). Fracture of femur simulation and photoelasticity analysis, Digest Journal of Nanomaterials and Biostructures, **8**(1): 177 – 185.

Liming Voo, Mehran Armand, and Michael Kleinberger. (2004). Stress Fracture Risk Analysis of the Human femur Based on Computational Biomechanics, Johns Hopkins Apl Technical Digest, **25**(3): 223-230.

Nithin Kumar KC, Tushar Tandon, Praveen Silori, Amir Shaikh. (2015). Biomechanical stress analysis of a Human femur bone using ANSYS, Materials Today: Proceedings 2,. 2115 – 2120.

Osteoporosis Fact Sheet. (2004). By International Osteoporosis Foundation Press release, 1-5. Retrieved on DATE:21/09/2018 from www.dolcera.com.

Ralph V.Mann and Amber Murphy, (2015). The Mechanics of Sprinting and Hurdling, 46-79.

Roesler H., (1987). The history of some fundamental concepts in bone biomechanics, J Biomech; **20**: 1025-34.

Rodrigues, H., Jacobs, C., Guedes, J.M. & Bendsoe, M.P. (1999). Global and local material optimization models applied to anisotropic bone adaptation, in Synthesis in Biosolid Mechanics. Vol 69. Kluwer Academic Publishers. 209-220.

Sandeep Das and Saroj Kumar S. (2014). "Finite Element Analysis of femur Fracture Fixation Plates", International Journal of Basic and Applied Biology, **1**(1): 1-5.

Utter, Brian. (2014). Experimental and computational techniques in soft condensed matter physics. Cambridge University Press; **9** - Photoelastic materials. **230-247.** doi. org/10.1017/CBO9780511760549.009; pp 230-247.

Vishay Precision Group. (2011). Introduction to stress analysis by the photo stress method, Tech Note: 11212/ TN-702-2. Retrieved on DATE:10/10/2018 from www. micro-measurements.com

Yousif A.E & Aziz, M.Y. (2012). Biomechanical analysis of the human femur bone during normal walking and standing up, IOSR Journal of Engineering, **2**(8): 13-19.

Submitted : 04/03/2019
Revised : 07/03/2019
Accepted : 27/04/2019

دراسة تجريبية عن التركيزات القصوى للإجهاد في عظام الفخذ من خلال نهج المرونة الضوئية

بروس رالفين روز
قسم الهندسة الميكانيكية، الحرم الإقليمي لجامعة آنا، تيرونيلفيلي، الهند

الملخص

يساعد التقدم في الطرق التجريبية لتحليل الإجهاد على فهم توزيع الإجهاد في هياكل العظام، وهو أمر ضروري لإجراء عمليات زراعة ناجحة. تتطلب الميكانيكا الحيوية منهجيات مهنية لحل المشكلات المعقدة حيث أن قياس التفاعلات الفيزيائية الناتجة عن الأحمال يكون ذو طابع غير عملي. في العمل الحالي، تم دراسة سلوك التوزيع الأقصى للإجهاد في عظام الفخذ البشري تحت تأثير الأحمال الثقيلة جداً التي تسببها الحوادث والأنشطة الرياضية من خلال نهج المرونة الضوئية. تم إجراء التجارب باستخدام منظار الاستقطاب الدائري عند أحمال إدخال وشروط حدية مختلفة. وتم حساب معامل تركيز الإجهاد من خلال الأوامر الهامشية المرتبطة بالإجهادات الناتجة من النموذج. وتم تطوير نموذج ثنائي الأبعاد لعظام الفخذ بمواد أكريليك لالتقاط نطاق الإجهاد عن طريق نهج الإضاءة البصرية. أظهر تحليل إجهاد المرونة الضوئية الحد الأقصى لإجهاد القص في مستوى سطح النموذج وفرق الجهد الرئيسي بموثوقية عالية. تم حساب مقادير الإجهاد الاسمية من الترتيب الهامشي من خلال البيانات التكميلية والتحليل العددي. وتم تسجيل وضع الإجهاد في عظام الفخذ في حالات مختلفة من خلال طرق عرض غير مباشرة ومتعددة من هوامش متسقة الألوان. طريقة تفسير الهامش الجديدة تعمل على تسهيل التعرف على المواد المناسبة للزراعة مع عامل أمان عالي في ظروف التحميل الفعلية.